Research on 3D Transient Electromagnetic Inversion Guided by One-Dimensional Resistivity Models

Mingyang Gong, Liangjun Yan, Xingbing Xie, Lei Zhou, Yurong Mao
Yangtze University, Wuhan, Hubei, China，yljemlab@163.com

SUMMARY

In order to meet the requirements of deep oil and gas exploration, groundwater and environmental monitoring, and geothermal exploration, high-precision and fast 3D inversion methods need to be developed for the Transient Electromagnetic method with electrical sources. Traditional methods of constructing initial models are time-consuming and subjective, posing significant challenges to inversion efficiency and data interpretation. Therefore, the rational construction of initial models is an urgent issue that needs to be addressed in current 3D inversion of Transient Electromagnetic methods. This study establishes a forward modeling under geological conditions, conducts inversion calculations using both a uniform half-space initial model and a one-dimensional resistivity-guided initial model construction method, and discusses the computational effects of both approaches. The results indicate that the inversion with a constrained initial model yields good results, providing an effective means for processing and interpreting actual data.

Keywords: Transient Electromagnetic Method, One-Dimensional Inversion, Initial Model, Three-Dimensional Inversion

INTRODUCTION

The Transient Electromagnetic method (TEM) with grounded-wire source is an important branch of controlled-source electromagnetic methods and has been widely used in environmental surveys, oil and gas exploration, mineral exploration, geothermal resource exploration, and deep crustal studies. As a crucial technology for exploring deep-seated mineral resources in the Earth, the working principle of the TEM with grounded-wire source involves transmitting a pulse signal underground using a long grounded-wire transmitter to achieve depth sounding. This method offers higher resolution and can overcome typical electromagnetic noise issues, providing richer electrical information about subsurface media in electromagnetic data interpretation. In recent years, there has been continuous advancement in the exploration technology of the Transient Electromagnetic method with electrical sources, with a growing demand for its applications.

Recently, rapid progress has been made in the development of 3D forward and inverse algorithms for Transient Electromagnetic methods, with some applications in simulation experiments and actual exploration. One-dimensional inversion allows for quick processing and quantitative interpretation. However, in regions with complex 3D electrical structures, one-dimensional inversion interpretations may lead to unreasonable geological models. Consequently, an increasing number of scholars are turning to two-dimensional and three-dimensional inversions for more detailed imaging of subsurface electrical structures. Foreign scholars have obtained frequency domain data from Fourier-transformed Transient Electromagnetic data and conducted 2.5D inversions using finite elements, obtaining electrical structures similar to Magnetotelluric (MT) data in shallow subsurface areas. Sasaki et al. (2015) developed a LOTEM 3D inversion algorithm based on the frequency-time domain transformation. Some researchers have considered the influence of topography and 3D underground structures, optimizing finite parameters of 3D models using stable damped least squares joint inversion methods to identify the resistivity characteristics of volcanic structures, leading to new insights into the geological conditions of the area. Cai et al. (2022) developed a two-dimensional joint inversion algorithm effectively coupling semi-airborne frequency domain electromagnetic data with long-offset Transient Electromagnetic data and applied the algorithm to geological interpretation near Schleiz in eastern Thuringia, Germany.

Moreover, addressing issues such as lateral continuity in one-dimensional Transient Electromagnetic inversion profiles, many scholars have begun researching the incorporation of lateral and spatial constraints into inversion techniques. Viezzoli et al. (2009) proposed spatially constrained inversion based on lateral constraints inversion. Yin Changchun et al. (2018) introduced bidirectional constraints into the spatially constrained inversion of the airborne electromagnetic pseudo three-dimensional model through regularization of a general measurement network, demonstrating the effectiveness of this method through theoretical and measured data inversions.

To improve the computational accuracy and reliability of inversion results, this paper discusses a strategy that involves using one-dimensional inversion results to guide the construction of a three-dimensional inversion initial model. By comparing the inversion effects of a uniform half-space initial model, the feasibility of this approach in enhancing inversion results has been validated.

METHODS

Inversion methods

In geophysical inversion problems, the objective function is typically composed of two parts:

$$\phi(\mathbf{m}) = \phi_d(\mathbf{m}) + \lambda\phi_m(\mathbf{m})$$
$$= \left\|\mathbf{W}_d\left(\mathbf{d}_{\text{obs}} - \mathbf{d}_{\text{pre}}\right)\right\|_2^2 + \lambda\|\mathbf{W}_m(\mathbf{m} - \mathbf{m}_{\text{ref}})\|_2^2. \quad (1)$$

In this context, $\phi_d(\mathbf{m})$ represents the data misfit term, $\phi_m(\mathbf{m})$ is the model constraint term; λ is the regularization factor; $\mathbf{m}$ is an N_m -dimensional model vector, where N_m is the number of model parameters; $\mathbf{m}_{\text{ref}}$ is the reference model determined based on prior information; $\mathbf{d}_{\text{obs}}$ is an N-dimensional vector of observed data, and $\mathbf{d}_{\text{pre}}$ represents predicted data; $\mathbf{W}_d$ is the weight matrix for measurement data errors; and $\mathbf{W}_m$ is the roughness matrix.

The LBFGS optimization method is employed to minimize the objective function. By using Equation (1) to derive the model parameters $\mathbf{m}$ and obtain the gradient of the objective function:

$$\mathbf{g}(\mathbf{m}) = -2\mathbf{J}^{\mathrm{T}}\mathbf{r} + 2\lambda\mathbf{W}_m^{\mathrm{T}}\mathbf{W}_m(\mathbf{m} - \mathbf{m}_{\text{ref}}). \quad (2)$$

Here, $\mathbf{J}$ is the sensitivity matrix $\mathbf{r} = \mathbf{W}_d^{\mathrm{T}}\mathbf{W}_d\left(\mathbf{d}_{\text{obs}} - \mathbf{d}_{\text{pre}}\right)$. By computing the transpose of the Jacobian matrix through adjoint forward modeling and multiplying it with the vector, $\mathbf{J}^{\mathrm{T}}\mathbf{r}$ can be obtained. This significantly reduces computational requirements and memory usage.

For the calculation of $\mathbf{J}^{\mathrm{T}}\mathbf{r}$, the forward equations can be written as:

$$\mathbf{AE} = \mathbf{b}. \quad (3)$$

Taking the derivative of Equation (3) with respect to the model parameters $\mathbf{m}$, we obtain:

$$\frac{\partial\mathbf{E}}{\partial\mathbf{m}} = \mathbf{A}^{-1}\left(\frac{\partial\mathbf{b}}{\partial\mathbf{m}} - \frac{\partial\mathbf{A}}{\partial\mathbf{m}}\mathbf{E}\right) = \mathbf{A}^{-1}\mathbf{G}, \quad (4)$$

The sensitivity matrix of the observed data can be expressed as:

$$\mathbf{J} = \frac{\partial\mathbf{d}_{\text{pre}}}{\partial\mathbf{m}} = \mathbf{Q}\frac{\partial\mathbf{E}}{\partial\mathbf{m}}. \quad (5)$$

Here, the interpolation operator $\mathbf{Q}$ can be written as $\mathbf{Q} = \mathbf{Q}_t\mathbf{Q}_d$, where $\mathbf{Q}_d$ is the matrix operator that interpolates the solution of the electric field to the measurement points, and $\mathbf{Q}_t$ is the matrix operator that interpolates the predicted data of the forward time channel to the observed time channel. Substituting Equations (4) and (5) into Equation (2) yields:

$$\mathbf{g}(\mathbf{m}) = -2\mathbf{G}^{\mathrm{T}}\mathbf{A}^{-\mathrm{T}}\mathbf{Q}^{\mathrm{T}}\mathbf{r} + 2\lambda\mathbf{W}_m^{\mathrm{T}}\mathbf{W}_m(\mathbf{m} - \mathbf{m}_{\text{ref}}) \quad (6)$$

This leads to the following adjoint forward equation:

$$\mathbf{A}^{\mathrm{T}}\mathbf{u} = \mathbf{Q}^{\mathrm{T}}\mathbf{r}. \quad (7)$$

After obtaining the vector $\mathbf{u}$ through reverse time iteration, it can be substituted into Equation (6) to obtain $\mathbf{J}^{\mathrm{T}}\mathbf{r}$, and subsequently calculate the gradient of the objective function.

For unstructured tetrahedral grids, the roughness matrix is constructed as follows:

$$W_m(i,j) = \begin{cases} -\sqrt{\dfrac{V_iV_{ij}}{V_{max}\sum_{k=1}^{N}V_{ik}}}\Big/ r_{ij} & i \neq j \\ -\displaystyle\sum_{j=1}^{N} W_m(i,j) & i = j \\ 0 & \text{else} \end{cases}. \quad (8)$$

Where N is the number of nearest neighboring elements; V_i is the volume of the i^{th} inversion element; V_{ij} is the volume corresponding to the j^{th} neighboring element of the i^{th} inversion element; V_{max} is the maximum volume of the inversion element; $\sum_{k=1}^{N}V_{ik}$ is the total volume of neighboring elements corresponding to the i^{th} inversion element; and r_{ij} is the Euclidean distance from the j^{th} neighboring element to the i^{th} inversion element.

RESULTS

Theoretical model

The three-dimensional layered spatial model is shown in Figure 1. The air resistivity is 10^8 Ω·m. The first layer is a high-resistivity cover layer with a resistivity of 1000 Ω·m and a thickness of 200 m.

The second layer has a resistivity of 200 Ω·m and a thickness of 200 m. The surrounding rock of the third layer has a resistivity of 100 Ω·m. A low-resistivity anomaly body with a resistivity of 10 Ω·m is buried at the center of the observation area, with dimensions of (1000 m, 1000 m, 400 m) and a burial depth of 1000 m. The grounded long wire source has a length of 2000 m and is located 2500 m from the center of the anomaly body. There are a total of 9 profiles with a spacing of 300 m between them. Each profile has 9 measurement points with a spacing of 300 m between them, totaling 81 measurement points. The observation time ranges from 0.1 ms to 0.1 s, calculating the electric field response of 101 time channels.

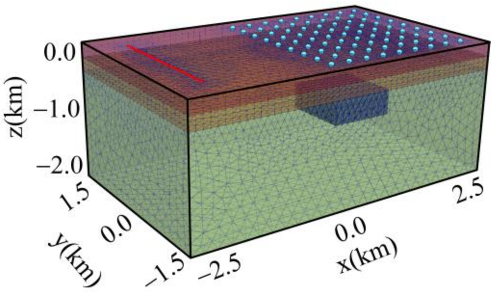

Figure 1. Theoretical model

Inversion results

Based on the forward modeling results, add 3% Gaussian noise, and conduct three-dimensional inversion using the synthesized forward data. Firstly, establish a uniform half-space with a background resistivity of 100 Ω·m. The inversion is iterated 96 times, with the RMS value decreasing from 33 to 1.4, taking a total of 20 hours. The inversion results are shown in the figure below.

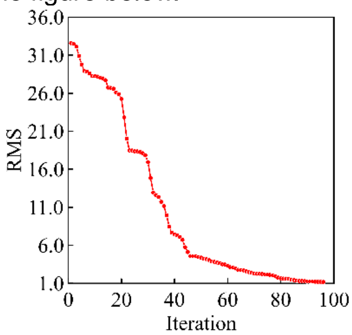

Figure 2. Data misfit

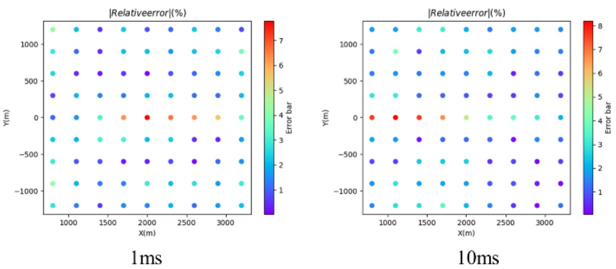

Figure 3. Data fitting situation

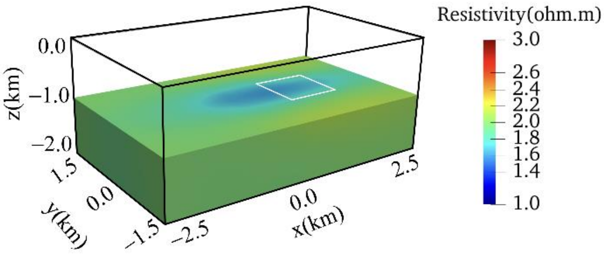

Figure 4. Inversion results

The second inversion calculation uses the one-dimensional inversion results to guide the establishment of a resistivity model as the initial model for inversion. The inversion is iterated 56 times, with the RMS value decreasing from 3.6 to 1.1, taking a total of 17 hours. The inversion results are shown in the figure below.

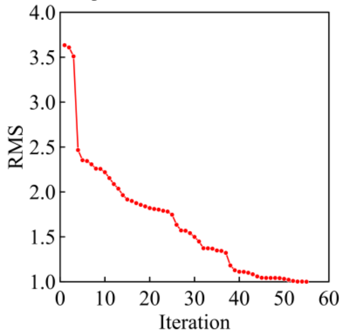

Figure 5. Data misfit

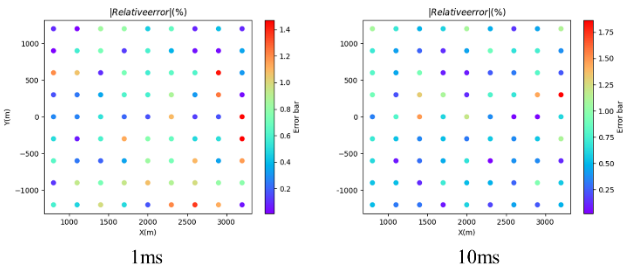

Figure 6. Data fitting situation

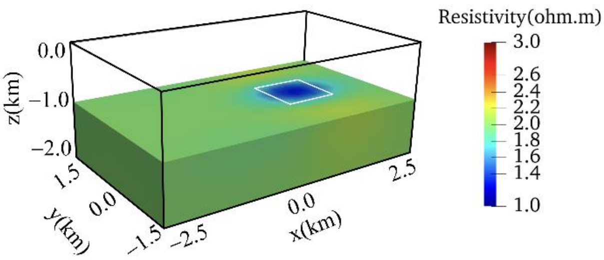

Figure 7. Inversion results

DISCUSSIONS

Comparing the above inversion results, both inversions can roughly reflect the distribution of the subsurface medium and the position and size of the anomaly body. However, there is a significant difference in their effectiveness, leading to the following conclusions:

1. When using a uniform half-space initial model for inversion, it can roughly reflect the position information and resistivity of the anomaly body, but there are still discrepancies compared to the true model. Additionally, the geological layer information is not fully recovered.
2. When using the one-dimensional resistivity initial model for inversion, the recovery of underground structural information is good, and it can more accurately reflect the position information and resistivity of the anomaly body.

CONCLUSIONS

Model experiments show that the layered structure of the subsurface has a significant impact on the recovery model of the inversion. When using a traditional uniform half-space initial model for inversion, the reflection of information about underground anomaly bodies is not accurate enough. This is mainly reflected in deviations in position information and resistivity values, leading to less reasonable underground electrical structures. On the other hand, when using the guidance of one-dimensional resistivity information to establish the initial resistivity model for inversion, the inversion results show good recovery of underground electrical structures and can more accurately reflect the position information and resistivity values of anomaly bodies. In actual exploration work, the geological structural environment in the survey area is often complex. Therefore, it is crucial to effectively utilize existing well seismic information and one-dimensional inversion layered structural information to establish a reasonable initial inversion model. The next step in the research will consider the influence of topographical factors and the inversion of field data.

ACKNOWLEDGEMENTS

This study was jointly funded by the National Natural Science Foundation of China, including the Key Program (42030805), the General Program (42274103), another General Program (42374091), the Youth Fund Project (42204079), and another General Program (42174083). We would also like to extend our gratitude to our fellow senior students who have provided valuable assistance.

REFERENCES

Cai J, Yogeshwar P, Mörbe W, et al. 2-D joint inversion of semi-airborne CSEM and LOTEM data in eastern Thuringia, Germany[J]. Geophysical Journal International, 2022, 229(3): 1475-1489

Sasaki Y, Yi M J, Choi J, et al. Frequency and time domain three-dimensional inversion of electromagnetic data for a grounded-wire source[J]. Journal of Applied Geophysics, 2015, 112: 106-114

Viezzoli A, Auken E, Munday T. Spatially constrained inversion for quasi 3d modelling of airborne electromagnetic data-an application for environmental assessment in the lower Murray region of south Australia[J]. Exploration Geophysics,. 2009, 40(2): 173-183

YIN ChangChun, ZHU Jiao, QIU ChangKai, CAI Jing. Spatially constrained inversion for airborne EM data using quasi-3D models. Chinese Journal of Geophysics (in Chinese),2018, 61(6): 2537-254